Korean J. Chem. Eng., 35(12), 2336-2347 (2018)
DOI: 10.1007/s11814-018-0149-y

pISSN: 0256-1115
eISSN: 1975-7220

Design and control of extractive distillation for the separation of methyl acetate-methanol-water

Honghai Wang, Pengyu Ji, Huibin Cao, Weiyi Su, and Chunli Li†

National-Local Joint Engineering Laboratory for Energy Conservation of Chemical Process Integration and Resources Utilization of Hebei University of Technology, Tianjin 300130, P. R. China
(*Received 5 June 2018 • accepted 3 September 2018*)

Abstract−The azeotrope of methyl acetate methanol and water was isolated using extractive distillation with water as entrainer. The pressure-swing extractive distillation (PSED) process and vapor side-stream distillation column (VSDC) with the rectifier process were designed to separate the methyl acetate, methanol and water mixture. It was revealed that the VSDC with the rectifier process had a reduction in energy consumption than the PSED process. Four control schemes of the two process were investigated: Double temperature control scheme (CS1), Q_R/F feedforward control of reboiler duty scheme for PESD (CS2), Q_R/F feedback control scheme for VSDC (CS3), the feedback control scheme of sensitive plate temperature of side-drawing distillation column to dominate the compressor shaft speed (CS4). Feed flow and composition disturbance were used to evaluate the dynamic performance. As a result, CS4 is a preferable choice for separation of methyl acetate-methanol-water mixture. A control scheme combining the operating parameters of dynamic equipment with the control indicators of static equipment was proposed in this paper. It means using the sensitive plate temperature of side-drawing column to control the compressor shaft speed. This is a new control scheme for extractive distillation.

Keywords: Extractive Distillation, Global Optimization, Energy Saving, Dynamic Control, Control Scheme

INTRODUCTION

Methyl acetate, an important organic solvent, is widely used in the pharmaceutical and textile industries. In fact, the wastewater from a pharmaceutical factory also contains a large amount of methyl acetate and methanol. If the wastewater is discharged directly, the component of methyl acetate and methanol will cause environmental pollution and waste of resources. Thus, the separation of methyl acetate/methanol is the key downstream process that determines the entire process economic benefits. However, methyl acetate and methanol form a binary minimum-boiling homogeneous azeotrope, so traditional distillation methods cannot achieve the mixture's separation effectively. Hence, other high efficiency technology should be developed for the separation of the binary azeotrope of methyl acetate and methanol.

There have been numerous researches on separating methyl acetate and methanol. Zheng et al. [1] converted methanol to methyl acetate by esterification reaction while the ratio of conversion was low and acetic acid may etch apparatus. Jie et al. [2] used ionic liquid as entrainer to separate the mixture. The research indicated that ionic liquid can substantially increase relative volatility and eliminate azeotropy. Therefore, ionic liquid can be treated as entrainer for the mixture. But ionic liquid is expensive so it is difficult to be used in industry [3]. The system also can be disposed by PVDF permeation and pervaporation membrane. When the content of methyl acetate is above 60 mol%, it selectively permeated methyl acetate, whereas the membrane may cause secondary pollution [4,5].

Extractive distillation as a special separation method is proposed for the separation of azeotropic system by adding another solvent [6,7]. Gao et al. [8] proposed the double solvent four column extractive distillation process, single solvent three column extractive distillation process and double solvent synergistic extractive distillation process, on the basis of screening the extraction agent for the system. Chen et al. [9] investigated a fully heat-integrated pressure swing distillation to separate methyl acetate and methanol. Many scholars improved the traditional distillation process by thermal integrated technology to reduce energy consumption, so it will improve the efficiency of energy [10,11].

The pressure-swing thermal coupling distillation investigated by Zhang et al. [12] can separate 24 different kinds of binary hydrocarbon mixtures with different boiling points. Then they calculated their cost-saving efficiency and compared with the conventional distillation column. The results showed that the heat coupling process was highly effective in reducing total cost.

Luyben [13] studied the controllability of conventional extractive distillation and thermal coupling extractive distillation for separating benzene/cyclohexane/toluene ternary mixtures with DMF as entrainer. The dynamics of a conventional separation process were compared with a thermally coupled process. The non-conventional process had lower energy cost than the conventional process, but its dynamic response to disturbances was worse.

This paper presents the PSED and VSDC with the rectifier to separate the mixture. The Aspen plus v7.2 version and Aspen dynamic v7.2 version were used in our research. NRTL model was

†To whom correspondence should be addressed.
E-mail: lichunli_hebut@126.com

selected to calculate the physical properties of system. The control schemes were designed based on response surface method (RSM) overall optimization. To prevent strong interaction among parameters, effective dynamic control structures were explored for the PSED process and VSDC with the rectifier process. The results of simulation and control structure will provide a fundamental guide for the industrialization design and production.

STEADY-STATE DESIGN

1. Design and Optimization of PSED Process

The pharmaceutical solvent wastewater was treated as the basic system for this work, and extractive distillation was used as the separation method. The fresh feed was 10,000 kg/h with composition of 74 wt% methyl acetate, 19 wt% methanol and 7 wt% water. Considering the water contained in feed, water was investigated as extractant.

As expected, the methyl acetate/methanol/water system is pressure-sensitive as methyl acetate getting azeotropic with methanol and water at 101.325 kPa. The total reflux distillation experiments

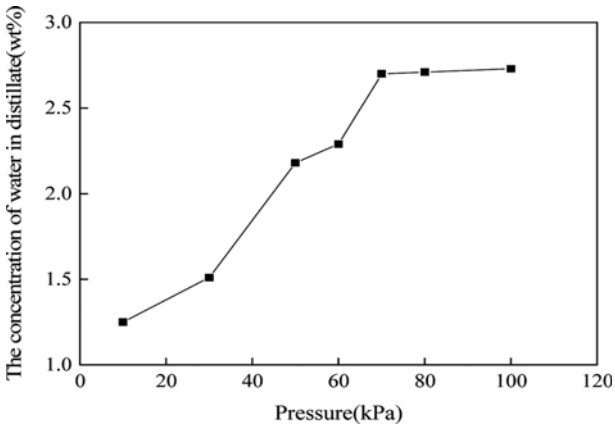

Fig. 1. The concentration of water in distillate at different pressure.

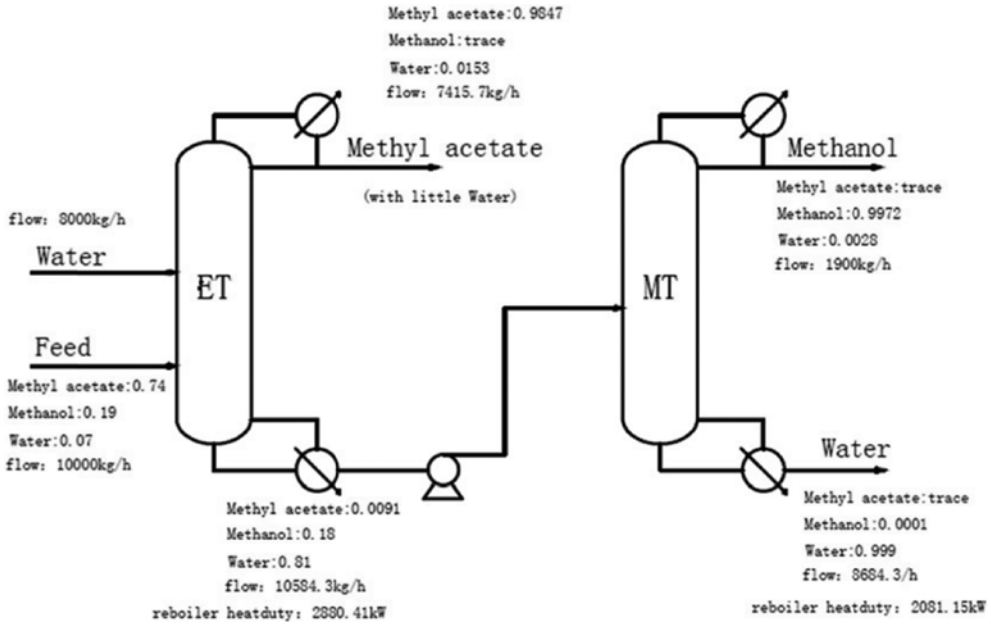

Fig. 2. Flowsheet of PSED.

Table 1. The comparison of optimization results for PSED

Case	Operating factors	Single factor	RSM
A	The number of therotical stage of ET	21	22
B	The solvent position of ET	11	10
C	The feed position of ET	16	17
D	The reflux ratio of ET	1.5	1.4
E	The solvent ratio (S/F) of ET	0.8	0.7
F	The therotical stage of MT	27	26
G	The feed position of MT	12	11
H	The reflux ratio of MT	2.0	1.9
Optimization results	The purity of methyl acetate	0.9847	0.9846
	The purity of methanol	0.9972	0.9967
	The total reboilers duty/kW	4961.56	4719.67

of methyl acetate and water were conducted under different pressure, as shown in Fig. 1; with the reduction of pressure, the water content reduced gradually. Considering the above condition, in the system, the extractive distillation operates at vacuum. The heavy entrainer can drag methanol into the bottom of the column. Then the bottom mixture gets a further separation in another column at normal pressure. The distillation process was simulated by Aspen Plus v7.2 with NRTL as the property method [14]. ET is the extractive distillation column which operates at 50 kPa, and MT is the methanol distillation column operating at normal pressure. The flowsheet is shown in Fig. 2.

Response surface method (RSM) is an optimization method based on statistics and mathematics. Based on single factor analysis of the process, central composite design (CCD) was designed. RSM was used for the global optimization for this process [15]. For PSED, the number of theoretical stage feed positions, solvent position, mass reflux ratio, solvent ratio and feed position, mass reflux ratio, the number of theoretical stage of MT served as operating parameters, while the purity of methyl acetate and the purity of methanol and the total reboiler duty served as main functions. As shown in Table 1, the operating condition optimized by RSM has an energy reduction of 4.88% compared to the single factor analysis results.

From results of RSM, the impact level of every factor on the objective functions and the final optimization results can be analyzed. From analyzing a large amount of data, the Fig. 3 is obtained. As given in Fig. 3(a), for the purity of methyl acetate, the order of influence degree is B>C>E>A>D>G>H>F, for methanol purity, B>H>C>E>A>G>D>F, for the reboiler duty, E>D>H>B>C>G>F>A, and as illustrated in Fig. 3(b), for the final results, B>E>D>C>H>A>G>F.

2. Design and Optimization of VSDC with the Rectifier

Fig. 4 shows the process of VSDC with the rectifier to separate the mixture [16]. The pressure of ET in this process is 50 kPa The methyl acetate and water obtained at the top of the ET. The purity

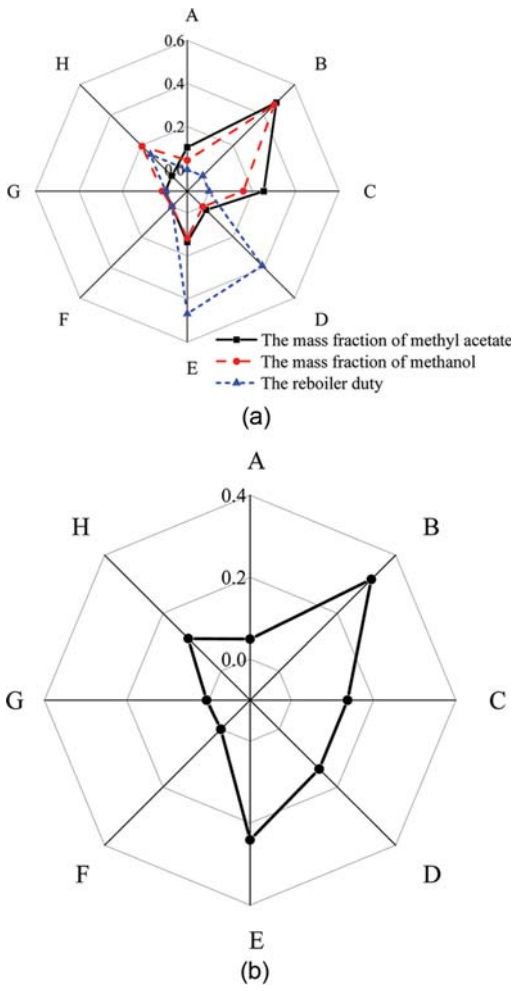

Fig. 3. The influence degree of each operating parameter on the objective functions and the optimization results. (a) The influence degree of parameter on the objective functions. (b) The influence degree of parameter on the optimization results.

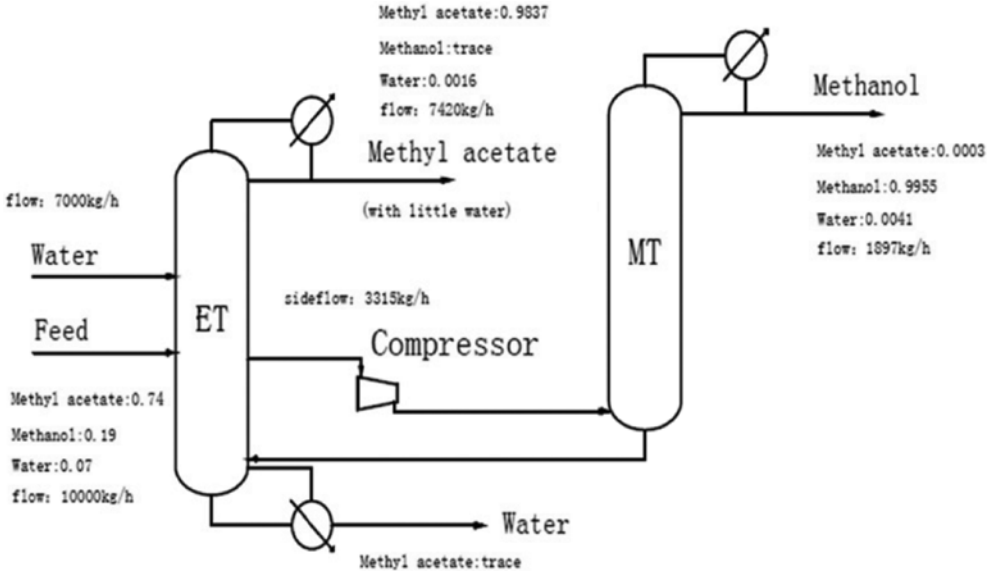

Fig. 4. VSDC with the rectifier.

Table 2. The comparison of optimization results for VSDC with the rectifier

Case	Operating factors	Single factor	RSM
A	The number of theoretical stage of ET	26	27
B	The solvent position of ET	10	9
C	The feed position of ET	16	17
D	The reflux ratio of ET	1.5	1.4
E_1	The side-product stage of ET	21	22
F_1	The side-product reflux of ET	21	22
G_1	The number of theoretical stage of MT	18	18
H	The reflux ratio of MT	1.5	1.5
	Side-product flow/kg	3315	3315
Optimization results	The purity of methyl acetate	0.9837	0.9837
	The purity of methanol	0.9955	0.9956
	Energy consumption/kW	4394.62	4303.47

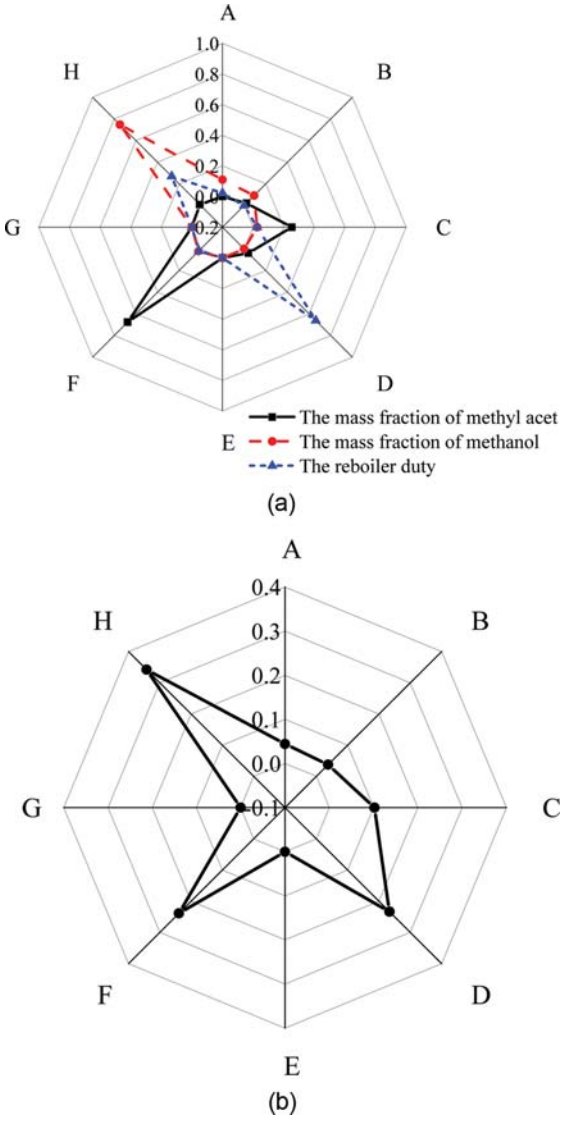

Fig. 5. The influence degree of each operating parameter on the objective functions and the optimization results. (a) The influence degree of parameter on the objective functions. (b) The influence degree of parameter on the optimization results.

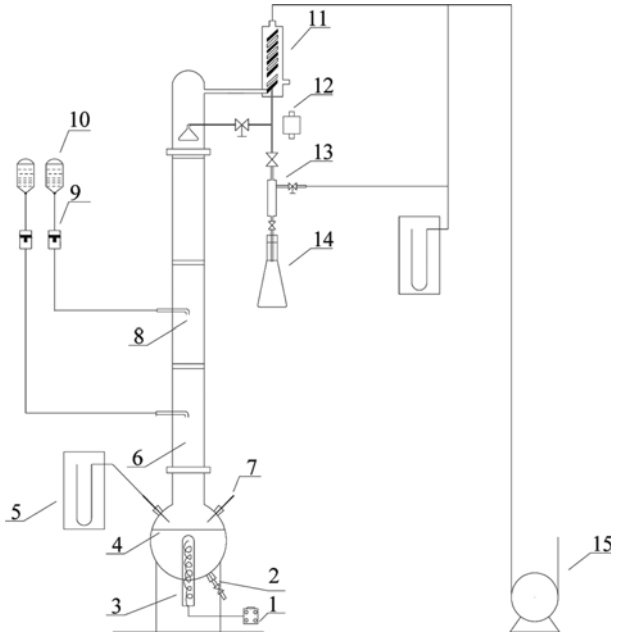

Fig. 6. Experimental devices of vacuum extractive distillation.

1. Heating furnace
2. Bottom valve
3. Electric heating
4. 3-Neck flash
5. Manometer
6. Main column
7. Thermometer
8. Feed inlet
9. Flowmeter
10. Solvent tank
11. Condenser
12. Regurgitant controller
13. Vacuum sampling tube
14. Top product collector
15. Circulating water pump

of methyl acetate and water is 98.37% and 1.63%. The side drawing vapor is transported to compressor to increase the pressure, so increasing the temperature and energy load of vapor makes the separation of methanol and water easier. MT operates at normal pressure which serves as rectifying section. The section below side-product stage serves as the public rectifying section. Methanol is obtained at the top of MT column.

First, the process is optimized by single factor analysis. Then the global optimization is analyzed by RSM. The results are given in

Table 3. Comparison of experiment results with simulation results at 50 kPa

Mass reflux ratio	1	1.5	2
Simulation	0.9831	0.9847	0.9848
Experiment	0.9187	0.9387	0.9486
Relative error/%	6.55	4.67	3.68

Table 2. The results has a 2.07% reduction of reboiler duty.

Also, the impact level of every factor on this process and the final optimization results can be analyzed from the results of RSM optimization. Fig. 5 is obtained by analyzing a large amount of data. As illustrated in Fig. 5(a), for the purity of methyl acetate, the rank of impact level is F_1>C>D>B>H>E_1>A>G_1, for methanol purity, H>A>B>C>F_1>G_1>E_1>D, for the reboiler duty, D>H>B>A>F_1>E_1, and as shown in Fig. 5(b), for the final results, H>F_1>D>C>A>B>E_1>G_1.

3. Experiment Verification

The experiment was used to make sure that the PSED to separate methyl acetate from the mixture is feasible. The laboratory equipment is shown in Fig. 6. The height of column is 1.5 m with diameter 30 mm, and it is packed with 3×3 metal θ rings. The column consisted of three sections with two feed inlets. According to the optimal conditions, each of the solvent feed position was at the middle of the second and third section.

The experiment was conducted at 25 °C with solvent ratio 0.7. The experiment results are given in Table 3. The experiment results coincide quite well with the simulation by relative error less than 7%.

CONTROL STRUCTURE DESIGN

1. Dynamic Simulation of Pressure-swing Extractive Distillation

1-1. Control Structure Analysis

The Aspen Plus simulation was switched to pressure-driven dynamic model when adding valve and device parameters. Considering the longer delay time and expensive equipment and high maintenance cost of component control structure, temperature control was chosen in the process. The temperature distribution in distillation column is actually the distribution of material concentration, which is influenced by operating pressure, temperature, feed state, flow rate, and so on. The temperature change of each plate can effectively determine whether the process is stable, especially the sensitive plate, which has the maximum temperature change and can monitor the operation process of the column to control the purity of the product. Adjusting the temperature of the sensitive plate can effectively prevent the light group from flowing to the bottom of the column and heavy group flowing to the top of the column. Effective relative gain array (ERGA) has better effect used in the process of variable pairs [17].

But in this paper, the singular value decomposition criterion used as the selection criterion for temperature control points for the system is not complicated.

Fig. 7(a) illustrates the open loop gain of each tray temperature for the reflux rate and the reboiler duty by the two input signals with

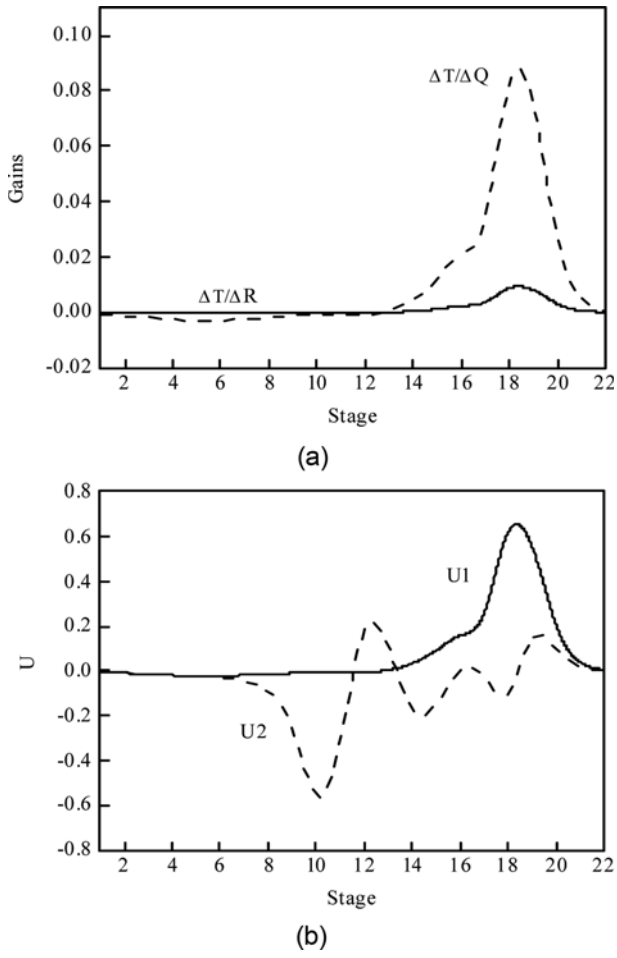

Fig. 7. Temperature sensitivity and SVD analysis of ET. (a) Temperature sensitivity analysis of ET. (b) SVD analysis of ET.

+0.1% change on the basis of steady-state values. As expected, the gain between the plate temperature and the reboiler duty is positive, and the gain between the plate temperature and the reflux flow is not obvious. It indicates that the reflux rate and reboiler duty are sensitive to temperature change of the eighteenth plate. Fig. 7(b) shows the vector value of U1 and U2 by singular values analysis, and the former is indicated by a solid line. The largest magnitude of U reflects the appropriate control stage [18]. The SVD analysis is similar with sensitive analysis in Fig. 7(a) that the temperature of 18 plate can be controlled by reflux rate and reboiler duty.

Fig. 8 shows the SVD analysis of MT. The analysis method is the same as above. The temperature of stage 10 is sensitive to reflux and reboiler duty, and stage 18 is sensitive to reboiler duty. The steady state gain matrix singular value $\sigma1$=0.0359, $\sigma2$=0.0042 and the condition number: $\sigma1/\sigma2$=8.5476. It is suitable to use double temperature control scheme for MT. In the paper, the double temperature control structure was developed on the basis of the control structures proposed by pioneers [19].

Extractive distillation process is a multi-input and multi-output process with complex operating conditions and multiple influencing factors [20]. It is necessary to satisfy the balance of material and energy in distillation process. In the control scheme, the flow con-

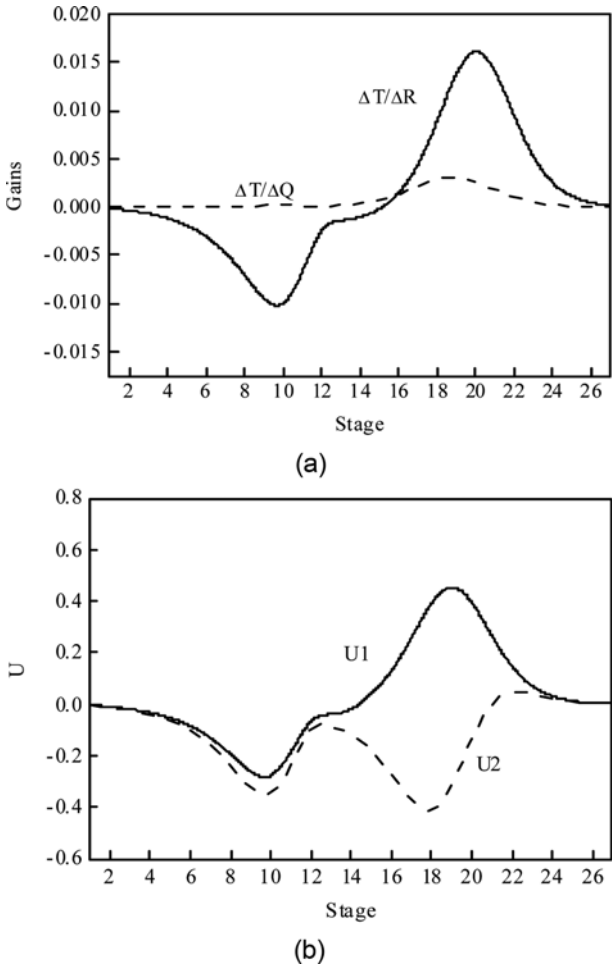

Fig. 8. Temperature sensitivity and SVD analysis of MT. (a) Temperature sensitivity of MT. (b) SVD analysis of MT.

trol, and the proportional control of the flow rate and feed flow are all based on the material balance. The reboiler duty and the reflux rate are based on the energy and material balance. The control of energy balance and material balance influences each other, while the sensitivity of energy balance control to component concentration is lower than that of material balance, but the response speed of material balance is slower. Therefore, it is better to adjust back flow and reboiler duty in the control structure if possible.

Hence, the detailed control structures are listed as follows:

(1) The operating pressure is controlled by condenser capacity;

(2) Feed flow is flow-controlled;

(3) The solvent flow rate is controlled with proportional control by the fixed solvent ratio;

(4) The vapor flow in column is controlled by the reboiler heat duty, the reboiler heat duty change as the feed changing.

(5) Reflux tank and reboiler levels are dominated by each product flow rate;

(6) The temperature of stage 18 in ET is controlled by reboiler duty;

(7) For MT, the temperature of stage 10 is controlled by reflux rate and stage 19 temperature by reboiler duty;

(8) The reflux rate of ET is the proportional control of feed flow

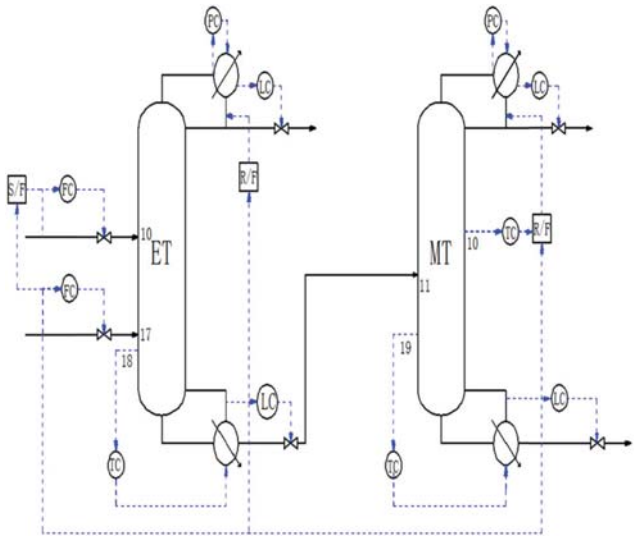

Fig. 9. Double temperature control structure (CS1).

rate with fixed signal of reflux to feed ratio.

1-2. Double Temperature Control Scheme (CS1)

The double temperature control scheme is shown in Fig. 9. The method of proportional control of ET reflux rate may mainly remain internal reflux unchanged and when the feed flow is stable. But when the feed flow increases, the reflux flow rate increases immediately at the first time. Therefore, the process of reaching stable state needs to overcome the relatively large disturbances.

In addition, the temperature of the stage 18 is controlled by the reboiler duty in reverse action. By the closed loop relay feedback test, the final gain is 0.78 and the integral time is 18.48 min.

The reflux flow has a fast speed of response to the changing of temperature with small hysteresis. It is effective to overcome the disturbance of feed in the distillation column. For the methanol column, the proportional control is proposed by the signals of the tenth plate temperature as well as the feed rate to control the back flow at the top. The temperature control is direct action with the gain 1.26 and the integral time 22.44 min. For T19, the gain is 0.968 and the integral is 18.48 min. The control parameters of CS1 is shown in Table 4.

1-3. Q_R/F Feedforward Control of Reboiler Duty Scheme (CS2)

In this research, the temperature control scheme was converted to Q_R/F control scheme with the cascade control of sensitive temperature and feed flow. Temperature acts as a feedforward of Q_R/F ratio to reduce energy fluctuation with reverse action. The main reason is that the reboiler duty can immediately decrease the re-

Table 4. CS1 control parameters

Controller	Gain	Integral time/min	Action
LC	2	999	Direct
FC/FSC	0.5	0.3	Reverse
T18	0.78	18.48	Reverse
T10	1.26	22.44	Direct
T19	0.968	18.48	Direct

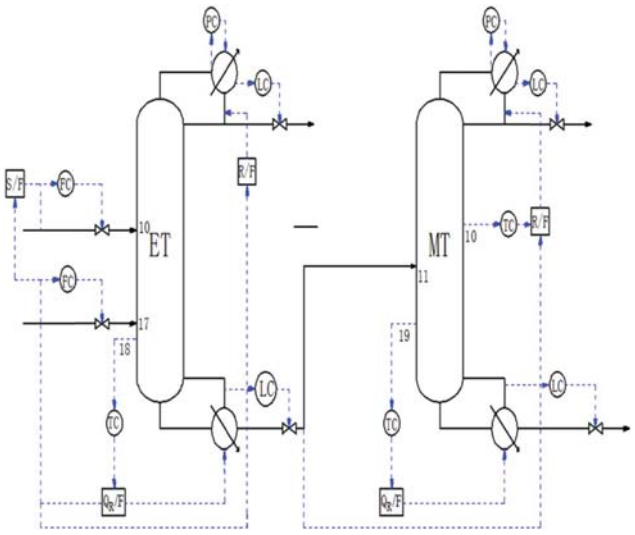

Fig. 10. Q_R/F feedback control of reboiler duty scheme (CS2).

Table 5. CS2 control parameters

Controller	Gain	Integral time/min	Action
LC	2	999	Direct
FC/FSC	0.5	0.3	Reverse
T18	0.54	19.9	Reverse
T10	1.26	22.44	Direct
T19	0.89	22.44	Direct

sponse of flow change as temperature changes. The scheme is shown in Fig. 10. The control parameters of CS2 are shown in Table 5.

1-4. The Comparison of Control Effect for CS1 and CS2

After the process operated for 1 h, ±10% disturbances of feed flow and composition was added to dynamic simulation. Methyl acetate was used as the composition disturbance, since the methyl acetate accounted for a large proportion in the composition of feed, the other components had less effect on the system. The goal was to ensure the purity of product to be stable at the fast speed and have small amplitude under disturbance. The control results comparison are as shown in Fig. 11.

With 10% disturbance of feed flow rate, for CS1, the purity of methyl acetate can be stable within 1 h, but the new stable value is less than the initial value with the overshoot 0.0003. But for CS2, the purity of methyl acetate can be stable in 0.6 h. The overshoot value is less than 0.0003.

For CS1, the content of methanol returns back to the initial value in 2 h, while the overshoot is 0.0055 with the minimum appoint reaching to 0.991, the product does not reach the standard. For CS2, the purity of methanol is stable in 1 h with the overshoot 0.0005, which is lower than that of CS1.

The temperature overshoot of T18 and T19 is all around 5 °C, so the control effect is not good. Thus, the impact on purity of product is larger with the stable time of 1 h and 3 h, respectively. For CS2, T18 can get to initial value within 1 h and the overshoot is only 0.5 °C, which is less than CS1 by 90%. Compared with CS1, the T19 stability time is shortened by 0.5 h. For CS2, the Q_{R1} stable time is shortened by 0.7 h and the overshoot is reduced by 0.2, whereas the overshoot of Q_{R2} is reductive and the stable time is the same as that of CS1.

The influence of the component disturbance on the system is shown in Fig. 11(b). CS2 has the same control effect with CS1 on the purity of methyl acetate with stable time in 0.5 h. For CS1, the purity of methanol is stable after 4 h and the initial value is less than 0.0027 with the purity of methanol less than 0.995 in 1 h. CS1 has a better effect with small amplitude and shorter stable time of 2 h.

Compared with the CS1 control scheme, as for the flow disturbance, it is obvious that the stable time of CS2 is shortened and the fluctuation amplitude is reduced. In the case of component disturbance, except the response of methanol purity, the other control effects of CS2 are the same as CS1. It is clear that the feedback control structure of Q_R/F has better control effect. Because the feed of MT is from the bottom of ET, in case of feed flow disturbance, the bottom flow disturbs at the first time, which in turn affects the operating conditions of methanol column. But the proportional control scheme of T19 and feed flow rate to adjust back flow of MT, to some extent, reduces the delayed response, so the operating parameters in MT can reach steady state faster.

2. Dynamic Simulation of VSDC with the Rectifier

2-1. Q_R/F Feedback Control Scheme (CS3)

Considering the complex interactions among variables in VSDC with the rectifier, temperature sensitivity plate is also analyzed by SVD method.

As illustrated in Fig. 12, plate 15 is the temperature-sensitive stage for reboiler duty and plate 18 for reflux rate. The singular values of the steady state gain matrix are $\sigma1$=0.0051 and $\sigma2$=0.001, which gives a conditional number of $\sigma1/\sigma2$=0.0051/0.001=5.1. It indicates that the interaction between two temperatures is not obvious, so a dual-temperature control scheme may be effective. The system is suitable for double temperature control. But considering stage 18 is far from the reflux drum compared with stage 15 and is close to the feed position, in the control structure, single temperature control scheme may be effective. For the rectifying section, sensitive plate is analyzed using temperature sensitivity criterion. The temperature of plate 13 is proposed to control the reflux rate.

VSDC with the rectifier is more complex than traditional two column. According to above research, Q_R/F has the better control effect. The energy of side rectifying section is provided by compressor. As researched by Wang [21], side-stream flow rate can be regulated to reject feed disturbance. The cascade control structure consists of proportion control for methanol purity in gas phase and the reboiler duty as well as the valve opening control for vapor mass flow. The cascade control can effectively main the flow stably. This is because the disturbance of feed may cause great disturbances for vapor flow rate and reboiler duty. The reboiler duty has a significant influence on the vapor flow rate and vapor phase composition of side-stream. Excessive vapor flow may cause a reduction of methanol purity, so that the purity of the product cannot reach the standard. Instead, the deficiency of flow may lead to the dissipation of a part of methanol at the bottom of the column, resulting in a waste of energy. The composition controller is used to maintain the content of methanol in vapor stream, and then we can

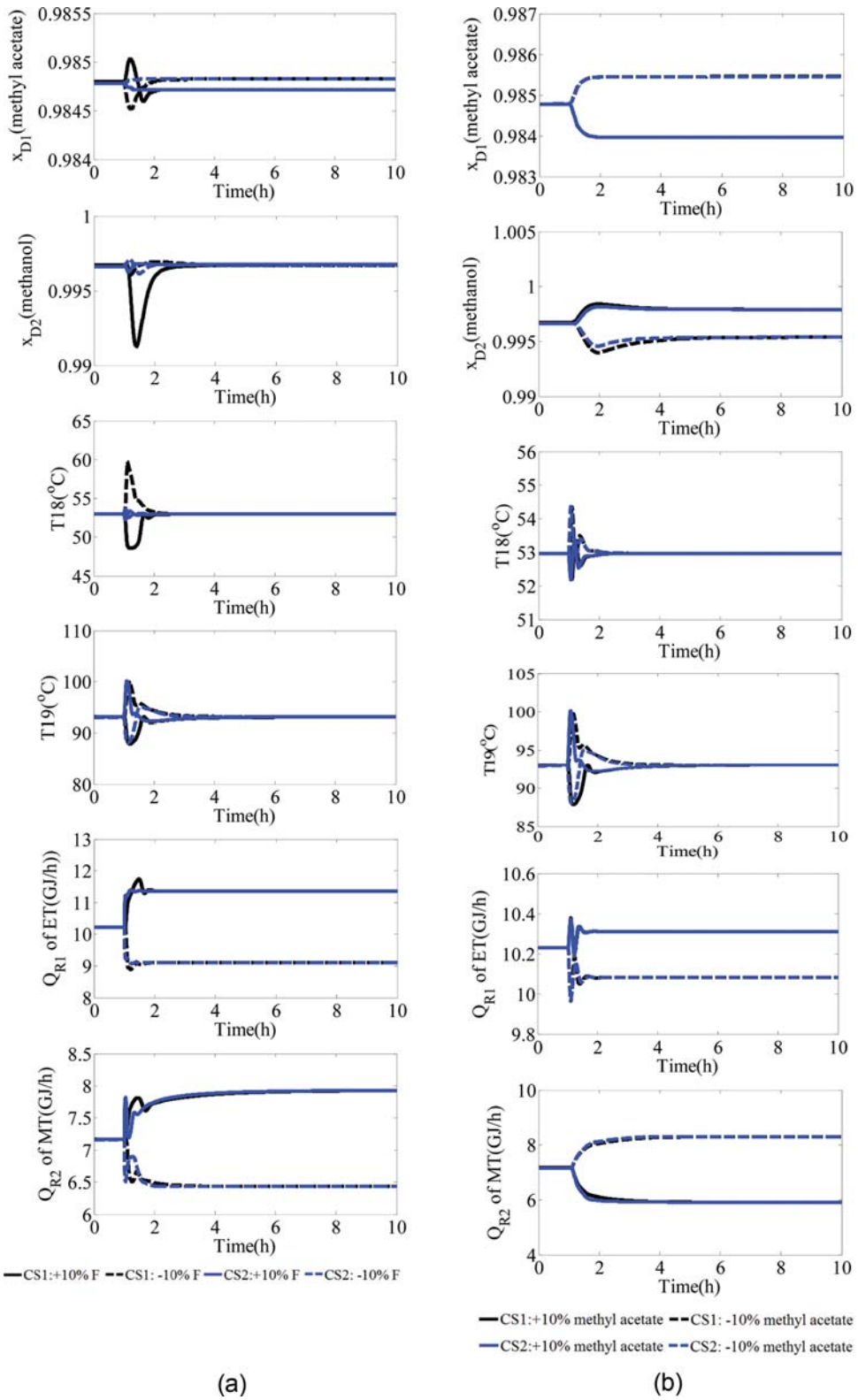

Fig. 11. Dynamic response comparison of CS1 and CS2. (a) Feed disturbance of ±10%. (b) Composition disturbance of ±10%.

ensure the methanol mass flow rate in side flow.

The cascade control structure of top product purity and T13 acting as the proportional signal for vapor mass flow can control the reflux rate of MT. In this scheme, a component controller is added to the rectifying column. Because, the plate temperature changes as the vapor flow disturbance. If the sensitive plate temperature can control the back flow and the temperature-component cascade control can maintain the purity of the product at a stable level, while

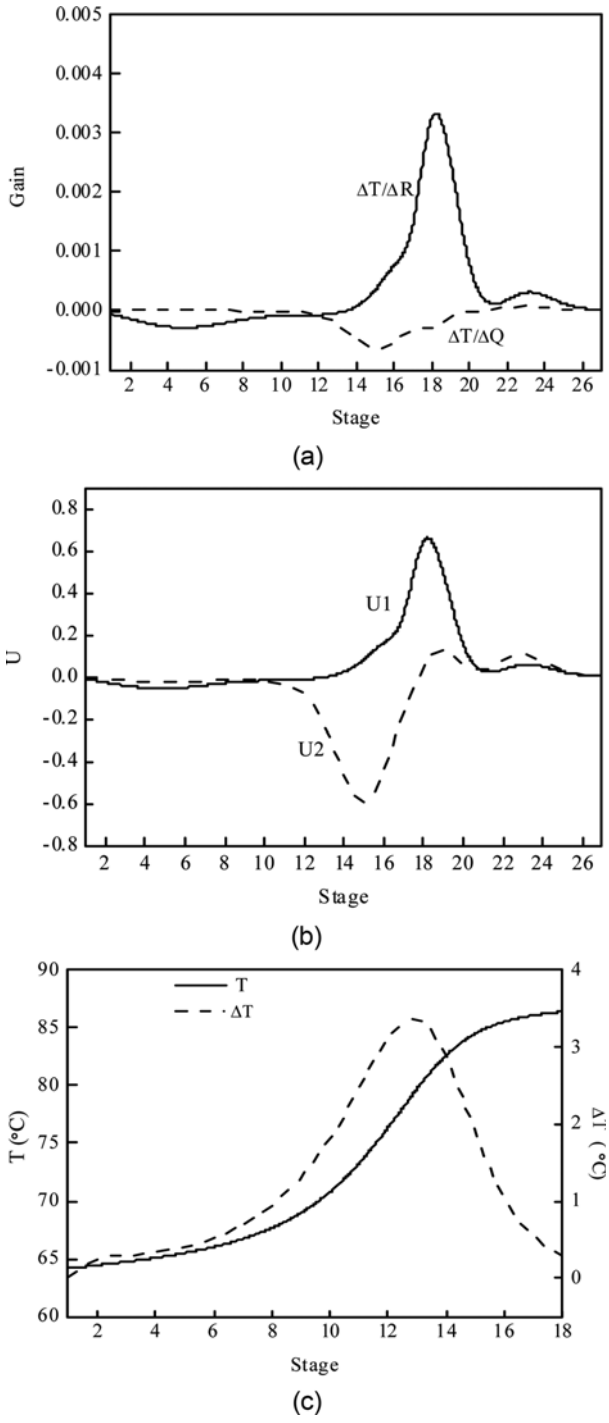

Fig. 12. Temperature sensitive stage analysis. (a) Temperature sensitivity of ET. (b) SVD analysis of ET. (c) Temperature sensitive stage analysis of MT.

the disturbance amplitude of product purity is relatively large. The control parameters are listed in Table 6 and the control scheme is shown in Fig. 13.

2-2. The Feedback Control Scheme of Sensitive Plate Temperature of Side Drawing Distillation Column to Dominate the Compressor Shaft Speed (CS4)

In CS3, the side-stream flow rate is dominated by valve, whereas

Table 6. CS3 control parameters

Controller	Gain	Integral time/min	Action
Liquid level	2	999	Direct
Feed flow	0.5	0.3	Reverse
Solvent flow	0.5	0.3	Reverse
T15	0.70	17.16	Reverse
T13	4.90	15.84	Direct
CC	23.48	75.24	Direct
VC	1	20	Direct

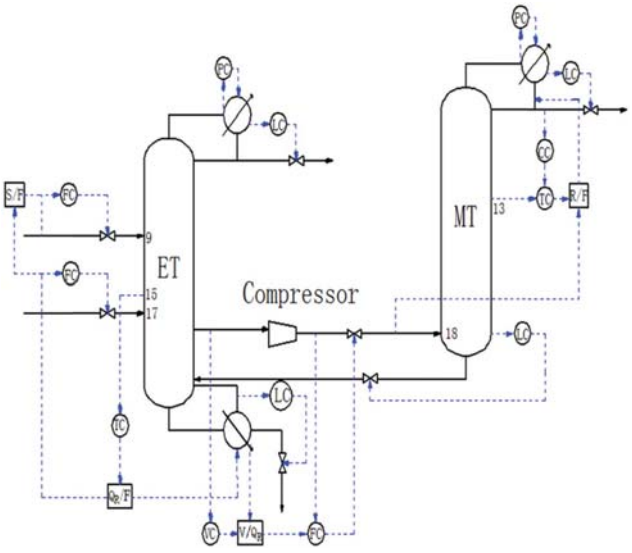

Fig. 13. CS3 control scheme of VSDC with the rectifier.

in CS4 we selected to control the compressor shaft speed by the sensitive plate temperature of the main column. CS4 with small fluctuations and shorter steady time is a new control scheme for the VSDC.

The SVD analysis of side-stream flow rate about the temperature sensitive plate of ET and MT was done. The results are shown in Fig. 14.

T23 and T13 are the temperature sensitive plates for ET and MT, respectively. But considering the side-stream position of 22 in ET, T23 cannot be used in the control structure because of the complex impact on both ET and MT by side reflux rate. In this paper, T13 was selected to dominate the shaft speed. In the feedback control structure, the compressor is controlled by T13 with a time delay of 1 min. The control flowsheet is shown in Fig. 15. The control parameters of CS4 are shown in Table 7.

2-3. The Comparison of Control Effect Comparison for CS3 and CS4

±10% feed flow rate and ±5% composition disturbance were utilized to test the controllability of CS3 and CS4. The methyl acetate was used as the composition disturbance, because the methyl acetate accounted for a large proportion in the composition of feed; the other components have less effect on the system. The control results are shown in Fig. 16.

When the flow rate is disturbed, the purity of methyl acetate in

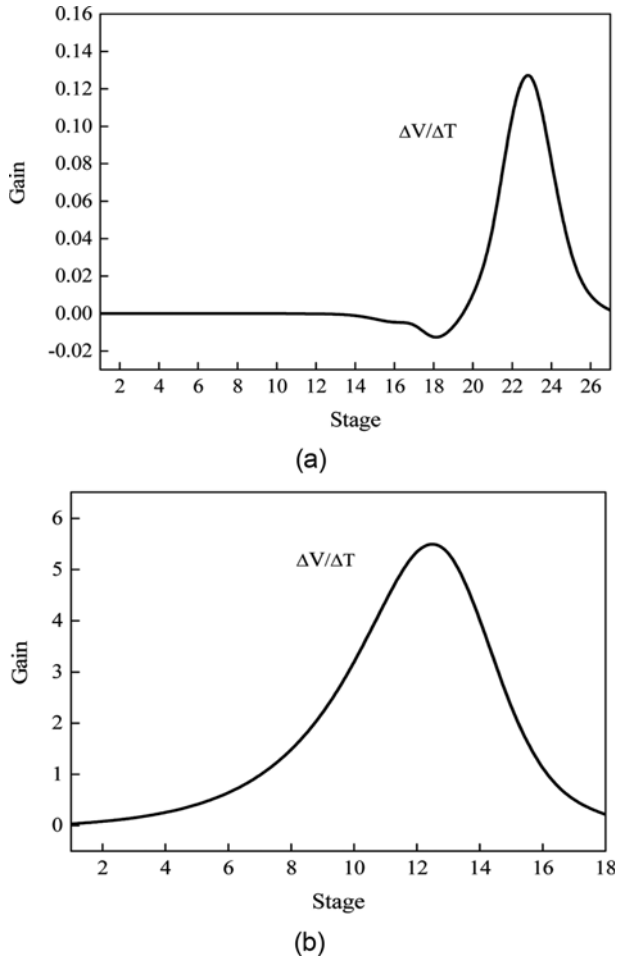

Fig. 14. Sensitivity analysis of sidedrawing flow rate. (a) Temperature sensitive stage analysis of ET. (b)Temperature sensitive stage analysis of MT.

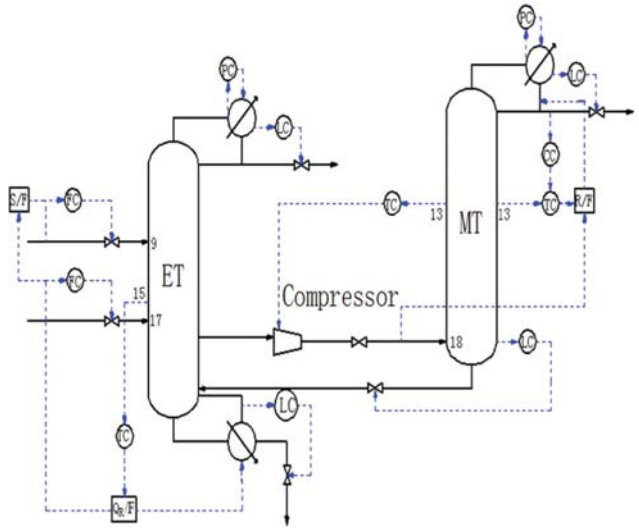

Fig. 15. CS4 control scheme of VSDC with the rectifier.

CS3 and CS4 can reach to stable value in 0.6 h. In CS3, the purity of methanol was stable within 2 h with the overshoot 0.003 and was less than 0.995 in 1 h. As for CS4, the process needed 3 h to recover to 0.995 with smaller amplitude. The heat duty reached a stable value at 2 h for CS3 and 0.5 h for CS4. The overshoot of CS4 was smaller than CS3. It indicated that it is better to control the compressor shaft speed instead of side-stream valve for the energy consumption in the process. Meanwhile, the side-stream flow rate of CS4 had the smaller overshoot and shorter steady time. In CS3 and CS4, T15 and T13 were stable within two hours, but T15 could recover to the initial value. While the steady state value of T13 was lower than the initial value.

Table 7. CS4 control parameters

Controller	Gain	Integral time/min	Action
LC	2	999	Direct
FC	0.5	0.3	Reverse
S/F	0.5	0.3	Reverse
T15	0.70	17.16	Reverse
T13	4.90	15.84	Direct
CC	23.48	75.24	Direct
VC	1	20	Direct
T13	1	20	Direct

Under the 5% disturbance of composition, the purity of methyl acetate and methanol came to a new value in 1 h and 3.5 h with smaller amplitude for CS4, respectively. But the steady time of CS4 was also longer than CS3. That is because the amplitude of vapor flow rate of CS4 was smaller than CS3, while the purity of methanol was sensitive to vapor flow rate. The less flow rate may lead to less methanol product. Thus, the recovery of methanol composition needs longer time. Compared with CS3, T15 and T13 of CS4 have the shorter steady time and smaller fluctuation. In CS4, Q_R can reach to the new value immediately and the amplitude is smaller.

Thus, for feed flow and composition disturbance, CS4 has better control effect than CS3 with less time to be stable and smaller amplitude. It indicates that the feedback control scheme of compressor shaft speed by the sensitive plate temperature of side drawing column is more suitable than CS3 for the process.

CONCLUSION

The extractive distillation process of methyl acetate-methanol-water using water as entrainer was investigated. Two methods for separating methyl acetate-methanol-water mixtures were explored. As the result, compared to the PSED, the VSDC with the rectifier process had 9.06% energy reduction. On the basis of the RSM global optimization, four control structures for distillation process with smaller fluctuation were studied. The feedback control scheme of sensitive plate temperature of side drawing distillation column to dominate the compressor shaft speed (CS4) is a new control scheme for extractive distillation.

(1) RSM global optimization is used in the optimization of the distillation process. Compared with single factor analysis, the PSED and VSDC with the rectifier had 4.88% and 2.07% energy reduction for reboiler duty, respectively.

(2) Considering both the energy consumption and controllabil-

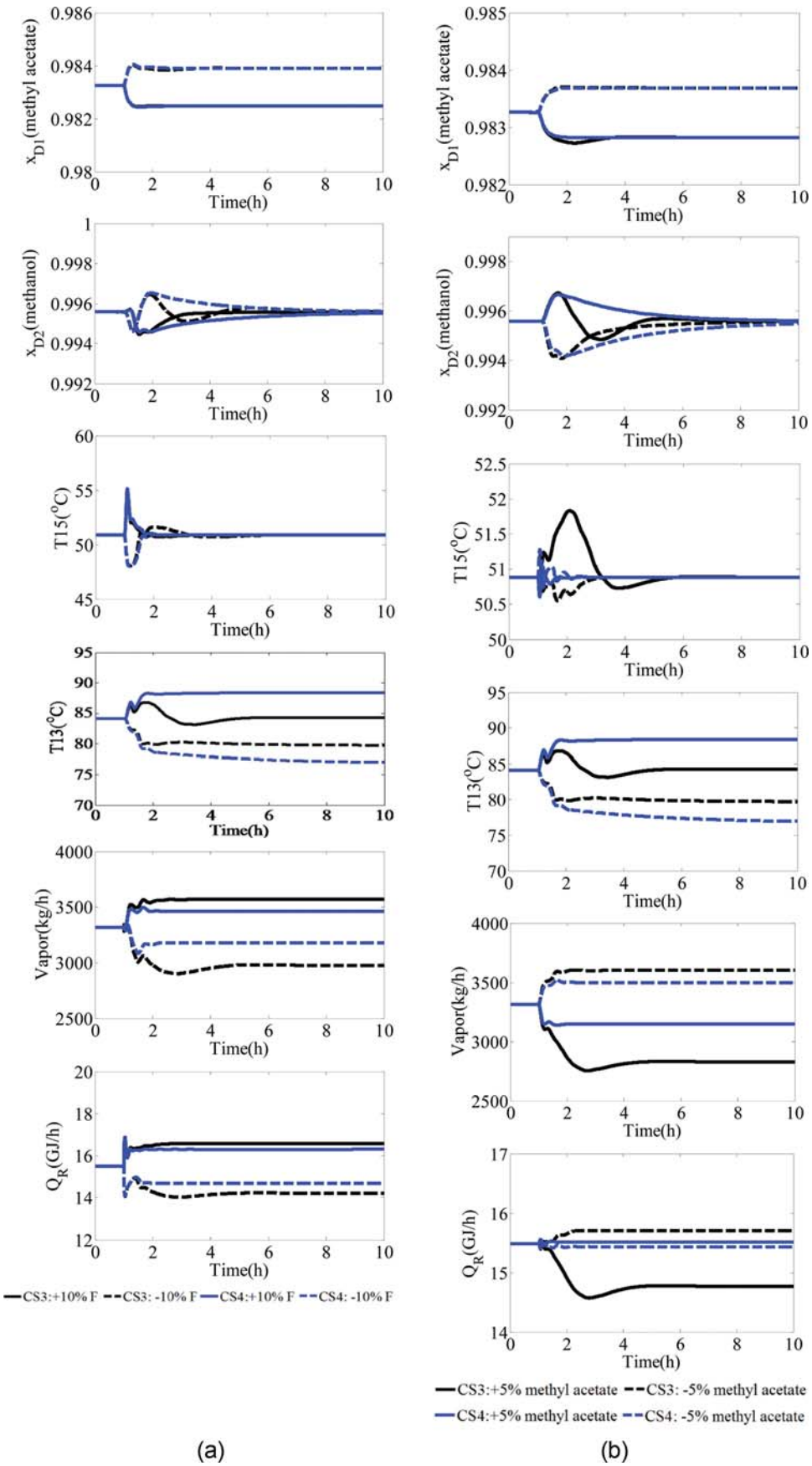

Fig. 16. Dynamic response comparison of CS3 and CS4. (a) Feed disturbance of ±10%. (b) Composition disturbance of ±5%.

ity, controlling the compressor shaft speed by the sensitive plate temperature of side drawing column (CS4) is a preferable choice for separation of methyl acetate-methanol-water mixture. A control scheme combining the operating parameters of dynamic equipment with the control indicators of static equipment was proposed in this paper. It means using the sensitive plate temperature of side drawing column to control the compressor shaft speed. This new type of control scheme with small fluctuations and shorter steady time is relatively uncommon in industry. In summary, we have further studied the process control scheme to maintain stable operation. It will reduce the additional energy consumption in operation process caused by instability.

ACKNOWLEDGEMENTS

This work was funded by the Applied Basic Research Program of Hebei Province, China [grant number: 16214505D].

NOMENCLATURE

CCD : central composite design
CS1 : double temperature control scheme
CS2 : Q_R/F feedforward control of reboiler duty scheme for PESD
CS3 : Q_R/F feedforward control scheme for VSDC
CS4 : the feedback control scheme of sensitive plate temperature of sidedrawing distillation column to dominate the compressor shaft speed
ET : extractive distillation column
F : feed flow rate, kg/h
MT : methanol recovery column
PSED : pressure-swing extractive distillation
Q_R : reboiler duty
R : mass reflux rate, kg/h
RSM : response surface method
S/F : solvent ratio
SVD : singular value decomposition
T : temperature [°C]
U : relative vector value in singular value decomposition
Vapor : side stream vapor flow rate [kg/h]
VSDC : vapor side-stream distillation column
ET : extractive distillation column
F : feed flow rate [kg/h]
MT : methanol recovery column
Q_R : reboiler duty
R : mass reflux rate [kg/h]
RSM : response surface method
S/F : solvent ratio
SVD : singular value decomposition
T : temperature [°C]
U : relative vector value in singular value decomposition
Vapor : side stream vapor flow rate [kg/h]

Greek Letters

σ : singular value

SUPPORTING INFORMATION

Additional information as noted in the text. This information is available via the Internet at http://www.springer.com/chemistry/journal/11814.

REFERENCES

1. H. Zheng, L. Xie, L. Cai, D. Wu and S. Zhao, *Chem. Eng. Process.*, **95**, 214 (2015).
2. H. Jie, X. Cui, Y. Peng, X. Li, L. Xu and R. Lin, *Huagong Xuebao/CIESC J.*, **67**, 606 (2016).
3. Z. Zhang, A. Hu, T. Zhang, Q. Zhang, M. Sun, D. Sun and W. Li, *Fluid Phase Equilib.*, **401**, 1 (2015).
4. G. Genduso, H. Farrokhzad, Y. Latré, S. Darvishmanesh, P. Luis and B. Van der Bruggen, *J. Membr. Sci.*, **482**, 128 (2015).
5. S. Lux, T. Winkler, M. Forstinger, S. Friesenbichler and M. Siebenhofer, *Sep. Sci. Technol.,* **50**, 2920 (2015).
6. V. Aniya, D. De and B. Satyavathi, *Ind. Eng. Chem. Res.*, **55**, 6982 (2016).
7. E. Hosgor, T. Kucuk, I. N. Oksal and D. B. Kaymak, *Comput. Chem. Eng.*, **67**, 166 (2014).
8. X. Gao, B. Zhu, Q. Gu, Y. Jiang and D. Yang, *Chin. J. Process. Eng.*, **17**(2), 254 (2017).
9. X. Chen, C. Liu and Z. Geng, *Chem. Eng. Process.*, **123**, 233 (2017).
10. W. L. Luyben, *Chem. Eng. Process.*, **107**, 29 (2016).
11. L. Li, Y. Tu, L. Sun, Y. Hou, M. Zhu, L. Guo, Q. Li and Y. Tian, *Ind. Eng. Chem. Res.*, **55**, 8837 (2016).
12. L. Zhang, J. Liu, X. Li, H. Li, B. Jiang and X. Xiao, *Sep. Sci. Technol.*, **50**, 148 (2015).
13. W. Luyben, *Chem. Eng. Res. Des.*, **106**, 253 (2016).
14. I. Navarro-Espinosa, C. Cardona and J. López, *Fluid Phase Equilib.*, **287**, 141 (2010).
15. H. Wang, X. Cui, C. Li and J. Fang, *Chem. Eng. Technol.*, **36**, 627 (2013).
16. W. L. Luyben, John Wiley & Sons, 292 (2013).
17. H. Wang, Y. Li, W. Su, Y. Zhang, J. Guo and C. Li, *Chem. Eng. Technol.*, **39**, 2339 (2016).
18. M. Xia, Y. Xin, J. Luo, W. Li, L. Shi, Y. Min and C. Xu, *Ind. Eng. Chem. Res.*, **52**, 17996 (2013).
19. W. Li, L. Shi, B. Yu, M. Xia, J. Luo, H. Shi and C. Xu, *Ind. Eng. Chem. Res.*, **52**, 7836 (2013).
20. W. Chang and I. Chien, *Ind. Eng. Chem. Res.*, **55**, 11291 (2016).
21. X. Wang, L. Xie, P. Tian and G. Tian, *Chem. Eng. Process.*, **110**, 172 (2016).

Supporting Information

Design and control of extractive distillation for the separation of methyl acetate-methanol-water

Honghai Wang, Pengyu Ji, Huibin Cao, Weiyi Su, and Chunli Li†

National-Local Joint Engineering Laboratory for Energy Conservation of Chemical Process Integration and Resources Utilization of Hebei University of Technology, Tianjin 300130, P. R. China
(*Received 5 June 2018 • accepted 3 September 2018*)

APPENDIX A

Table S1. The design of CCD and simulation results of pressure-swing extractive distillation

Run	Variables								Simulation results		
	A	B	C	D	E	F	G	H	MAC	MC	QR
1	20	10	15	1.4	0.7	28	11	2.1	0.9971	0.9941	5195973
2	19.3	11	16	1.5	0.8	27	12	2	0.9954	0.9832	5311255
3	20	10	15	1.6	0.9	26	11	1.9	0.9978	0.9834	5452685
4	20	12	15	1.4	0.7	28	11	1.9	0.9944	0.9812	5068745
5	22	12	17	1.6	0.7	28	13	1.9	0.9978	0.9929	5245169
6	22	12	15	1.4	0.7	28	13	2.1	0.9946	0.9821	5184790
7	20	10	17	1.6	0.7	26	11	1.9	0.9973	0.9932	5248203
8	21	11	17.7	1.5	0.8	27	12	2	0.9974	0.9935	5309244
9	22	12	17	1.4	0.9	26	13	2.1	0.9978	0.9948	5369414
10	20	12	17	1.6	0.7	26	13	2.1	0.9967	0.9887	5357985
11	22	12	15	1.6	0.9	26	13	2.1	0.9968	0.9888	5542089
12	22	12	17	1.4	0.7	26	11	1.9	0.9977	0.9944	5068600
13	22	10	17	1.6	0.7	28	11	2.1	0.9979	0.9956	5367819
14	22	12	17	1.6	0.9	28	11	2.1	0.9979	0.9932	5546317
15	22	10	15	1.6	0.7	28	13	1.9	0.9978	0.9955	5251330
16	20	12	17	1.6	0.9	26	11	1.9	0.9973	0.9809	5442806
17	21	11	16	1.5	0.8	27	14	2	0.9978	0.9949	5309726
18	22	10	15	1.4	0.7	26	11	1.9	0.9972	0.9929	5079851
19	20	12	15	1.4	0.7	26	11	2.1	0.9944	0.9813	5181177
20	21	11	14.3	1.5	0.8	27	12	2	0.9956	0.9839	5311581
21	20	10	17	1.4	0.7	26	13	2.1	0.9971	0.9954	5190608
22	20	12	15	1.4	0.7	26	13	1.9	0.9943	0.982	5065605
23	21	11	16	1.5	0.8	28.7	12	2	0.9978	0.995	5313104
24	20	12	15	1.6	0.9	28	13	1.9	0.9966	0.9792	5444411
25	22	12	15	1.6	0.7	26	11	1.9	0.9949	0.9815	5240665
26	21	11	16	1.67	0.8	27	12	2	0.9978	0.9934	5483451
27	22	10	17	1.6	0.7	26	13	2.1	0.9979	0.9956	5364634
28	22	10	15	1.4	0.9	26	13	2.1	0.9977	0.9969	5376682
29	21	11	16	1.5	0.8	27	12	2	0.9978	0.995	5309540
30	20	10	15	1.6	0.7	26	13	2.1	0.9976	0.9945	5364432
31	21	11	16	1.5	0.8	27	12	2	0.9978	0.995	5309540
32	22	10	17	1.6	0.9	28	13	2.1	0.9979	0.9957	5552367
33	22.7	11	16	1.5	0.8	27	12	2	0.9979	0.9952	5309632
34	21	12.7	16	1.5	0.8	27	12	2	0.9960	0.9857	5303699

Table S1. Continued

Run	Variables								Simulation results		
	A	B	C	D	E	F	G	H	MAC	MC	QR
35	21	11	16	1.5	0.8	25.3	12	2	0.9978	0.9948	5306171
36	21	11	16	1.5	0.8	27	12	2	0.9978	0.995	5309540
37	21	11	16	1.5	0.8	27	12	2	0.9978	0.995	5309540
38	20	10	17	1.6	0.9	28	11	2.1	0.9975	0.9938	5552990
39	20	10	17	1.6	0.9	26	13	1.9	0.9975	0.9828	5451409
40	21	11	16	1.5	0.63	27	12	2	0.9972	0.9924	5125066
41	21	11	16	1.5	0.8	27	12	1.8	0.9978	0.9876	5204887
42	20	10	15	1.4	0.9	28	13	1.9	0.9976	0.9842	5285629
43	22	10	17	1.4	0.7	28	13	1.9	0.9978	0.9978	5079255
44	22	10	17	1.6	0.9	26	11	2.1	0.9979	0.9949	5549702
45	20	12	17	1.4	0.7	28	11	2.1	0.9965	0.9896	5186843
46	20	12	17	1.4	0.9	28	13	1.9	0.9972	0.9819	5273757
47	22	12	15	1.4	0.9	26	11	1.9	0.9964	0.9771	5271997
48	22	10	15	1.4	0.9	28	11	2.1	0.9977	0.9945	5385180
49	21	11	16	1.5	0.97	27	12	2	0.9979	0.9797	5521350
50	21	11	16	1.5	0.8	27	12	2	0.9978	0.995	5309540
51	21	11	16	1.5	0.8	27	12	2	0.9978	0.995	5309541
52	21	9.32	16	1.5	0.8	27	12	2	0.9977	0.9966	5322753
53	20	12	15	1.6	0.7	28	11	2.1	0.9947	0.9806	5359770
54	21	11	16	1.33	0.8	27	12	2	0.9974	0.9952	5139630
55	22	10	17	1.6	0.9	28	11	1.9	0.9979	0.983	5457569
56	21	11	16	1.5	0.8	27	12	2.2	0.9978	0.995	5426044
57	22	12	15	1.4	0.9	28	13	1.9	0.9964	0.9782	5274142
58	20	10	17	1.4	0.9	26	11	1.9	0.9974	0.9823	5283666
59	21	11	16	1.5	0.8	27	10.3	2	0.9978	0.9925	5313880
60	20	12	15	1.4	0.9	28	13	2.1	0.9962	0.9887	5371043

Table S2. Regression analysis of methyl acetate composition

Source	Sum of squares	df	Mean square	F value	P-value Prob>F
Model	6.29E-05	44	1.43E-06	11.35	<0.0001
A-A	2.56E-06	1	2.56E-06	20.28	0.0004
B-B	1.19E-05	1	1.19E-05	94.62	<0.0001
C-C	6.24E-06	1	6.24E-06	49.51	<0.0001
D-D	5.60E-07	1	5.60E-07	4.44	0.0523
E-E	3.36E-06	1	3.36E-06	26.69	0.0001
F-F	4.46E-09	1	4.46E-09	0.035	0.8534
G-G	3.44E-08	1	3.44E-08	0.27	0.609
H-H	2.83E-08	1	2.83E-08	0.22	0.6427
AB	9.22E-08	1	9.22E-08	0.73	0.4058
AC	3.58E-07	1	3.58E-07	2.84	0.1125
AD	3.37E-12	1	3.37E-12	2.67E-05	0.9959
AE	1.09E-08	1	1.09E-08	0.087	0.7727
AF	5.66E-09	1	5.66E-09	0.045	0.8351
AG	3.72E-11	1	3.72E-11	2.95E-04	0.9865
AH	1.53E-07	1	1.53E-07	1.21	0.2881
BC	4.63E-06	1	4.63E-06	36.74	<0.0001
BD	3.66E-09	1	3.66E-09	0.029	0.867
BE	1.24E-06	1	1.24E-06	9.84	0.0068

Table S2. Continued

Source	Sum of squares	df	Mean square	F value	P-value Prob>F
BF	1.61E-08	1	1.61E-08	0.13	0.7261
BG	4.32E-08	1	4.32E-08	0.34	0.5672
BH	1.68E-08	1	1.68E-08	0.13	0.7201
CD	9.29E-08	1	9.29E-08	0.74	0.4041
CE	8.26E-07	1	8.26E-07	6.55	0.0218
CF	3.53E-08	1	3.53E-08	0.28	0.6044
CG	1.14E-07	1	1.14E-07	0.9	0.3574
CH	4.33E-08	1	4.33E-08	0.34	0.5666
DE	2.20E-09	1	2.20E-09	0.017	0.8965
DF	1.32E-09	1	1.32E-09	0.01	0.92
DG	2.77E-07	1	2.77E-07	2.2	0.1588
DH	5.79E-09	1	5.79E-09	0.046	0.8332
EF	5.35E-15	1	5.35E-15	4.25E-08	0.9998
EG	6.70E-09	1	6.70E-09	0.053	0.8208
EH	7.99E-09	1	7.99E-09	0.063	0.8046
FG	2.68E-13	1	2.68E-13	2.13E-06	0.9989
FH	3.22E-09	1	3.22E-09	0.026	0.8752
GH	1.73E-08	1	1.73E-08	0.14	0.7161
A^2	1.74E-06	1	1.74E-06	13.78	0.0021
B^2	1.04E-06	1	1.04E-06	8.27	0.0116
C^2	2.37E-06	1	2.37E-06	18.83	0.0006
D^2	8.65E-09	1	8.65E-09	0.069	0.7969
E^2	3.53E-10	1	3.53E-10	2.80E-03	0.9585
F^2	1.52E-07	1	1.52E-07	1.21	0.2893
G^2	1.52E-07	1	1.52E-07	1.21	0.2893
H^2	1.52E-07	1	1.52E-07	1.21	0.2893
Residual	1.89E-06	15	1.26E-07		
Lack of fit	1.89E-06	10	1.89E-07		
Pure error	0	5	0		
Cor total	6.48E-05	59			

Table S3. Regression analysis of methanol composition

Source	Sum of squares	df	Mean square	F value	P-value Prob>F
Model	0.002190052	44	4.97739E-05	7.87334875	<0.0001
A-A	3.55782E-05	1	3.55782E-05	5.62783195	0.0315
B-B	0.00038289	1	0.00038289	60.5663703	<0.0001
C-C	0.0001297	1	0.0001297	20.5162792	0.0004
D-D	1.50184E-06	1	1.50184E-06	0.2375645	0.6330
E-E	9.66844E-05	1	9.66844E-05	15.2937577	0.0014
F-F	5.01204E-09	1	5.01204E-09	0.00079282	0.9779
G-G	1.29232E-05	1	1.29232E-05	2.04422238	0.1733
H-H	0.00015952	1	0.00015952	25.2332547	0.0002
AB	5.51655E-07	1	5.51655E-07	0.08726206	0.7717
AC	7.21085E-06	1	7.21085E-06	1.14062828	0.3024
AD	8.36703E-07	1	8.36703E-07	0.13235149	0.7211
AE	3.58626E-07	1	3.58626E-07	0.05672832	0.8150
AF	1.77719E-06	1	1.77719E-06	0.28112062	0.6037
AG	6.03147E-08	1	6.03147E-08	0.00954072	0.9235

Table S3. Continued

Source	Sum of squares	df	Mean square	F value	P-value Prob>F
AH	3.37265E-07	1	3.37265E-07	0.05334926	0.8205
BC	6.43642E-05	1	6.43642E-05	10.1812751	0.0061
BD	4.79955E-08	1	4.79955E-08	0.00759203	0.9317
BE	2.95131E-05	1	2.95131E-05	4.66844828	0.0473
BF	2.13495E-09	1	2.13495E-09	0.00033771	0.9856
BG	6.5809E-08	1	6.5809E-08	0.01040981	0.9201
BH	3.31852E-06	1	3.31852E-06	0.52493112	0.4799
CD	2.38129E-06	1	2.38129E-06	0.37667808	0.5486
CE	1.17794E-05	1	1.17794E-05	1.86329806	0.1924
CF	1.3105E-07	1	1.3105E-07	0.02072984	0.8874
CG	5.0957E-06	1	5.0957E-06	0.80604895	0.3835
CH	2.91383E-07	1	2.91383E-07	0.04609166	0.8329
DE	1.19473E-06	1	1.19473E-06	0.18898463	0.6700
DF	7.52383E-08	1	7.52383E-08	0.01190136	0.9146
DG	1.4906E-06	1	1.4906E-06	0.23578674	0.6343
DH	1.06053E-06	1	1.06053E-06	0.16775756	0.6879
EF	3.89175E-08	1	3.89175E-08	0.00615606	0.9385
EG	1.44013E-07	1	1.44013E-07	0.02278022	0.8820
EH	0.000165978	1	0.000165978	26.2547059	0.0001
FG	4.42151E-07	1	4.42151E-07	0.06994049	0.7950
FH	5.90163E-07	1	5.90163E-07	0.0933533	0.7642
GH	1.22794E-06	1	1.22794E-06	0.19423763	0.6657
A^2	2.89703E-05	1	2.89703E-05	4.58259327	0.0491
B^2	6.18363E-06	1	6.18363E-06	0.97814068	0.3383
C^2	3.75144E-05	1	3.75144E-05	5.93411645	0.0278
E^2	0.000101206	1	0.000101206	16.0089646	0.0012
F^2	9.49872E-06	1	9.49872E-06	1.50252965	0.2392
G^2	1.69005E-06	1	1.69005E-06	0.26733583	0.6127
H^2	5.12544E-06	1	5.12544E-06	0.81075341	0.3821
Residual	9.48273E-05	15	6.32182E-06		
Lack of fit	9.48273E-05	10	9.48273E-06		
Pure error	0	5	0		
Cor total	0.002284879	59			

Table S4. Regression analysis of total reboiler duty

Source	Sum of squares	df	Mean square	F value	P-value Prob>F
Model	9.50794E+11	44	21608944325	85.1273215	<0.0001
A-A	235752.2213	1	235752.2213	0.00092873	0.9761
B-B	658409286.2	1	658409286.2	2.59376942	0.1281
C-C	64521389.71	1	64521389.71	0.25417869	0.6215
D-D	2.21161E+11	1	2.21161E+11	871.251173	<0.0001
E-E	2.66634E+11	1	2.66634E+11	1050.39173	<0.0001
F-F	28240113.41	1	28240113.41	0.11125047	0.7433
G-G	37700039.76	1	37700039.76	0.14851736	0.7054
H-H	80658112613	1	80658112613	317.748474	<0.0001
AB	1457133.642	1	1457133.642	0.0057403	0.9406
AC	11765437.48	1	11765437.48	0.04634933	0.8324
AD	52066580.54	1	52066580.54	0.20511361	0.6571

Table S4. Continued

Source	Sum of squares	df	Mean square	F value	P-value Prob>F
AE	45047704.12	1	45047704.12	0.17746311	0.6795
AF	67039215.99	1	67039215.99	0.26409753	0.6148
AG	160764.1986	1	160764.1986	0.00063332	0.9803
AH	119411744.1	1	119411744.1	0.47041641	0.5033
BC	55900875.03	1	55900875.03	0.22021861	0.6456
BD	5184337.953	1	5184337.953	0.02042343	0.8883
BE	3132189.903	1	3132189.903	0.0123391	0.9130
BF	3894424.856	1	3894424.856	0.01534189	0.9031
BG	77573.92566	1	77573.92566	0.0003056	0.9863
BH	207579.2109	1	207579.2109	0.00081775	0.9776
CD	4203279.631	1	4203279.631	0.0165586	0.8993
CE	32765902.66	1	32765902.66	0.12907958	0.7244
CF	58098377.33	1	58098377.33	0.22887556	0.6393
CG	60344492.17	1	60344492.17	0.23772401	0.6329
DE	6439321.285	1	6439321.285	0.02536737	0.8756
DF	5841792.015	1	5841792.015	0.02301344	0.8814
DG	2349236.981	1	2349236.981	0.0092547	0.9246
DH	85993702.68	1	85993702.68	0.33876776	0.5692
EF	3630625.615	1	3630625.615	0.01430266	0.9064
EG	23068828.69	1	23068828.69	0.09087846	0.7672
EH	342367789.2	1	342367789.2	1.34874024	0.2636
FG	379443.3662	1	379443.3662	0.0014948	0.9697
FH	975414.4028	1	975414.4028	0.00384259	0.9514
GH	2086816.103	1	2086816.103	0.0082209	0.9290
A^2	2642823.89	1	2642823.89	0.01041127	0.9201
B^2	6281500.945	1	6281500.945	0.02474565	0.8771
C^2	2794617.51	1	2794617.51	0.01100925	0.9178
D^2	11.23120117	1	11.23120117	4.4245E-08	0.9998
E^2	300308283.9	1	300308283.9	1.18304899	0.2939
F^2	7966922.61	1	7966922.61	0.03138528	0.8618
G^2	154574.5217	1	154574.5217	0.00060894	0.9806
H^2	34011227.05	1	34011227.05	0.13398547	0.7194
Residual	3807639652	15	253842643.5		
Lack of fit	3807639652	10	380763965.2		
Pure error	0	5	0		
Cor total	9.54601E+11	59			

Table S5. The related parameters of the fitted models of objective function

Parameter	Value		
	MAC	MC	QR
Std.Dev.	3.550E-004	2.514E-003	15932.44
R-Squared	0.9708	0.9585	0.9960
Adj R-Squared	0.8853	0.8368	0.9843
Pred R-Squared	−1.4013	−2.0862	0.8096
Adeq Precision	12.998	9.819	36.582

APPENDIX B

Table S1. The design of CCD and simulation results of external thermal coupling extractive distillation

Run	Variables								Simulation results		
	A	B	C	D	E	F	G	H	MAC	MC	QR
1	25	11	17	1.6	20	20	18	1.6	0.99314	0.9780	4596558
2	26	10	14	1.5	21	21	17	1.5	0.9964	0.9901	4694728
3	25	11	15	1.6	20	22	16	1.6	0.9970	0.9903	4787258
4	27	9	17	1.6	22	22	16	1.4	0.9978	0.9978	4792888
5	25	9	17	1.4	22	20	16	1.4	0.9936	0.9597	4627638
6	24	10	16	1.5	21	21	17	1.5	0.9977	0.9561	4795708
7	25	11	15	1.4	22	22	18	1.6	0.9965	0.9882	4618298
8	27	11	17	1.6	22	22	16	1.6	0.9977	0.9984	4595398
9	27	9	17	1.6	22	20	16	1.6	0.9935	0.9795	4619288
10	26	10	16	1.5	21	21	17	1.5	0.9975	0.9959	4690948
11	25	9	17	1.6	20	20	16	1.4	0.9943	0.9607	4796628
12	25	11	15	1.4	20	20	16	1.6	0.9958	0.9898	4429908
13	26	10	16	1.5	21	22.7	17	1.5	0.9971	0.9747	4547301
14	27	11	17	1.6	20	22	18	1.4	0.9977	0.9741	4780198
15	26	10	16	1.5	21	21	17	1.5	0.9975	0.9959	4690948
16	26	10	16	1.5	19.3	21	17	1.5	0.9975	0.9958	4691053
17	25	9	15	1.4	20	22	16	1.6	0.9970	0.9936	4631278
18	26	12	16	1.5	21	21	17	1.5	0.9964	0.9877	4686069
19	27	9	15	1.4	22	22	16	1.6	0.9973	0.9966	4450138
20	27	9	17	1.6	20	20	18	1.6	0.9934	0.9793	4609118
21	27	9	15	1.4	22	20	18	1.6	0.9967	0.9944	4454188
22	26	10	16	1.5	21	21	17	1.5	0.9975	0.9959	4690948
23	27	9	17	1.6	20	22	16	1.6	0.9977	0.9986	4610568
24	25	11	17	1.6	22	20	16	1.4	0.9940	0.9563	4785488
25	25	9	17	1.4	20	20	18	1.6	0.9927	0.9761	4448668
26	27	9	17	1.4	20	22	18	1.4	0.9973	0.9767	4624858
27	27	9	17	1.6	22	22	18	1.6	0.9978	0.9990	4609838
28	25	11	15	1.4	20	22	16	1.4	0.9965	0.9511	4626328
29	26	10	16	1.5	21	21	17	1.5	0.9975	0.9959	4690948
30	28	10	16	1.5	21	21	17	1.5	0.9976	0.9763	4786288
31	25	11	17	1.4	20	22	16	1.6	0.9976	0.9936	4616388
32	27	11	15	1.4	20	22	18	1.6	0.9970	0.9954	4596488
33	26	10	16	1.5	21	21	17	1.5	0.9975	0.9959	4690948
34	25	11	15	1.4	20	20	18	1.4	0.9959	0.9661	4608788
35	27	11	17	1.4	20	20	16	1.4	0.9933	0.9557	4618658
36	27	11	15	1.4	22	22	18	1.4	0.9965	0.9694	4612888
37	26	10	16	1.5	21	21	17	1.7	0.9963	0.9918	4499238
38	27	11	15	1.6	20	20	16	1.4	0.9963	0.9683	4782828
39	26	8	16	1.5	21	21	17	1.5	0.9969	0.9950	4551268
40	26	10	17.7	1.5	21	21	17	1.5	0.9931	0.9788	4534068
41	27	11	15	1.4	22	20	16	1.4	0.9962	0.9683	4782778
42	26	10	16	1.33	21	21	17	1.5	0.9968	0.9948	4370628
43	26	10	16	1.5	21	21	15	1.5	0.9975	0.9973	4528488
44	25	9	15	1.6	22	20	16	1.4	0.9974	0.9748	4789108
45	26	10	16	1.5	23	21	17	1.5	0.9975	0.9976	4538770
46	27	11	17	1.4	22	20	18	1.6	0.9924	0.9750	4442568
47	25	9	15	1.4	22	22	18	1.4	0.9970	0.9559	4639538

Table S1. Continued

Run	Variables								Simulation results		
	A	B	C	D	E	F	G	H	MAC	MC	QR
48	26	10	16	1.5	21	21	19	1.5	0.9975	0.9951	4691788
49	25	9	17	1.6	22	22	16	1.6	0.9978	0.9976	4794678
50	25	11	15	1.6	22	22	18	1.4	0.9970	0.9525	4794408
51	26	10	16	1.7	21	21	17	1.5	0.9977	0.9949	4862808
52	25	9	17	1.6	22	20	18	1.4	0.9943	0.9599	4745558
53	26	10	16	1.5	21	19	17	1.5	0.9936	0.9772	4700148
54	27	9	15	1.4	20	20	16	1.4	0.9967	0.9942	4444528
55	26	10	16	1.5	21	21	17	1.5	0.9975	0.9959	4690948
56	26	10	16	1.5	21	21	17	1.3	0.9975	0.9528	4704328
57	25	9	15	1.6	20	20	18	1.6	0.9973	0.9970	4604328
58	25	11	17	1.4	22	22	18	1.4	0.9976	0.9553	4623918
59	27	9	15	1.6	20	22	18	1.4	0.9978	0.9765	4793208
60	27	11	15	1.6	22	20	18	1.6	0.9963	0.9679	4782378

Table S2. Regression analysis of methyl acetate composition

Source	Sum of squares	df	Mean square	F value	P-value Prob>F
Model	1.47E-04	21	7.00E-06	120.54	<0.0001
A-A	4.86E-09	1	4.86E-09	0.084	0.7739
B-B	1.84E-06	1	1.84E-06	31.76	<0.0001
C-C	2.15E-05	1	2.15E-05	370.7	<0.0001
D-D	3.31E-06	1	3.31E-06	56.93	<0.0001
E-E	8.04E-09	1	8.04E-09	0.14	0.7119
F-F	5.75E-05	1	5.75E-05	990.18	<0.0001
G-G	2.18E-10	1	2.18E-10	3.75E-03	0.9515
AC	2.14E-07	1	2.14E-07	3.69	0.0622
BC	1.00E-06	1	1.00E-06	17.24	0.0002
BD	3.13E-07	1	3.13E-07	5.39	0.0257
BF	2.59E-07	1	2.59E-07	4.47	0.0412
CF	2.88E-05	1	2.88E-05	496.04	<0.0001
CH	5.71E-07	1	5.71E-07	9.84	0.0033
FH	3.51E-07	1	3.51E-07	6.05	0.0186
A^2	7.27E-07	1	7.27E-07	12.51	0.0011
B^2	4.25E-07	1	4.25E-07	7.31	0.0102
C^2	1.23E-05	1	1.23E-05	212.1	<0.0001
E^2	3.93E-07	1	3.93E-07	6.77	0.0132
F^2	6.80E-06	1	6.80E-06	117.04	<0.0001
G^2	3.93E-07	1	3.93E-07	6.77	0.0132
Residual	2.21E-06	38	5.81E-08		
Lack of fit	2.21E-06	33	6.69E-08		
Pure error	0	5	0		
Cor total	1.49E-04	59			

Table S3. Regression analysis of methanol composition

Source	Sum of squares	df	Mean square	F value	P-value Prob>F
Model	0.013768899	27	0.000509959	31.3718051	<0.0001
A-A	0.000669014	1	0.000669014	41.1565645	<0.0001
B-B	0.000559165	1	0.000559165	34.3988601	<0.0001
C-C	0.000162234	1	0.000162234	9.98036725	0.0034
D-D	1.93004E-07	1	1.93004E-07	0.01187327	0.9139
E-E	6.01521E-06	1	6.01521E-06	0.37004501	0.5473
F-F	0.000133044	1	0.000133044	8.18462007	0.0074
G-G	6.67393E-06	1	6.67393E-06	0.41056875	0.5262
H-H	0.004538033	1	0.004538033	279.171897	<0.0001
AB	0.000141117	1	0.000141117	8.68130176	0.0060
AF	0.000156938	1	0.000156938	9.65455569	0.0039
AH	0.000628757	1	0.000628757	38.68006	<0.0001
BC	8.55073E-05	1	8.55073E-05	5.26025884	0.0285
BF	0.000136204	1	0.000136204	8.37906049	0.0068
BG	5.00866E-05	1	5.00866E-05	3.08124265	0.0888
BH	6.83647E-05	1	6.83647E-05	4.20567919	0.0486
CD	9.80895E-05	1	9.80895E-05	6.03429683	0.0196
CF	0.000552521	1	0.000552521	33.9901308	<0.0001
EH	4.73415E-05	1	4.73415E-05	2.91236509	0.0976
FH	0.000223833	1	0.000223833	13.7698054	0.0008
A^2	0.00125569	1	0.00125569	77.2478666	<0.0001
C^2	6.69451E-05	1	6.69451E-05	4.11834451	0.0508
D^2	5.40062E-05	1	5.40062E-05	3.32236654	0.0777
E^2	0.000102244	1	0.000102244	6.28989588	0.0174
F^2	0.000435787	1	0.000435787	26.808854	<0.0001
G^2	8.77017E-05	1	8.77017E-05	5.39525609	0.0267
H^2	0.000693072	1	0.000693072	42.6365634	<0.0001
Residual	0.000520171	32	1.62553E-05		
Lack of fit	0.000520171	27	1.92656E-05		
Pure error	0	5	0		
Cor total	0.01428907	59			

Table S4. Regression analysis of reboiler duty

Source	Sum of squares	df	Mean square	F value	P-value Prob>F
Model	5.4952E+11	9	61057779631	12.8789437	<0.0001
A-A	12302269325	1	12302269325	2.59492296	0.1135
B-B	14265184167	1	14265184167	3.00896143	0.0890
D-D	3.58556E+11	1	3.58556E+11	75.6302895	<0.0001
E-E	74585083.57	1	74585083.57	0.01573226	0.9007
F-F	10342533877	1	10342533877	2.18155512	0.1459
H-H	1.46059E+11	1	1.46059E+11	30.8082152	<0.0001
AF	18139453837	1	18139453837	3.8261628	0.0561
EF	24090216841	1	24090216841	5.0813598	0.0286
A^2	26457505297	1	26457505297	5.58069297	0.0221
Residual	2.37045E+11	50	4740899638		
Lack of fit	2.37045E+11	45	5267666265		
Pure error	0	5	0		
Cor total	7.86565E+11	59			

Table S5. The related parameters of the fitted models of objective function

Parameter	Value		
	MAC	MC	QR
Std.Dev.	2.410E-004	4.032E-003	68854.19
R-Squared	0.9852	0.9636	0.6986
Adj R-Squared	0.9770	0.9329	0.6444
Pred R-Squared	0.9610	0.8588	0.5691
Adeq Precision	36.918	18.943	14.993